Fuel 122 (2014) 223–228

Contents lists available at ScienceDirect

Fuel

journal homepage: www.elsevier.com/locate/fuel

Measurement and prediction of high-pressure viscosities of biodiesel fuels

Samuel V.D. Freitas [a], José J. Segovia [b], M. Carmen Martín [b], Johnny Zambrano [b,d], Mariana B. Oliveira [a], Álvaro S. Lima [c], João A.P. Coutinho [a,*]

[a] CICECO, Chemistry Department, University of Aveiro, Campus de Santiago, 3810-193 Aveiro, Portugal
[b] Grupo de Investigación TERMOCAL-Termodinámica y Calibración, Universidad de Valladolid, Paseo del Cauce 59, 47011 Valladolid, Spain
[c] Universidade Tiradentes, Av. Murilo Dantas 300, Farolândia, Aracaju-SE, Brazil
[d] Escuela Politécnica Nacional, Facultad de Ingeniería en Geología y Petróleos, Departamento de Petróleos, Ladrón de Guevara E11-253, Quito, Ecuador

HIGHLIGHTS

- New experimental η data for 3 biodiesels (293.15–393.15 K; 0.1–140 MPa).
- A correlation was proposed to predict the experimental data with OARDs of only 3.9%.
- Biodiesel + diesel mixtures η were predicted with OARDs of just 3.3%.

ARTICLE INFO

Article history:
Received 8 October 2013
Received in revised form 13 December 2013
Accepted 8 January 2014
Available online 22 January 2014

Keywords:
Biodiesel
Viscosity
High-pressure
Grundberg–Nissan rules
Biodiesel–diesel blends

ABSTRACT

Nowadays common rail injection systems use high pressures to pump the fuel, even if at these conditions the liquid viscosity increases substantially over atmospheric levels. For the proper operation of these injection systems the knowledge of fuels high-pressure viscosities becomes crucial to optimize the engine performance. This work reports new experimental data of high-pressure viscosities for three biodiesels (soybean, rapeseed and their binary mixture) measured at temperatures from 293.15 K to 393.15 K and pressures from atmospheric up to 140 MPa, and proposes a correlation capable of describing the experimental data. The predictions results are excellent for the biodiesels studied, presenting overall average relative deviations (OARD) of only 3.9% in the entire ranges of pressures and temperatures studied. This correlation was also extended to describe the viscosities of biodiesels mixtures with diesel with an OARD of just 3.3%.

1. Introduction

Biodiesel is a mixture of alkyl esters obtained from vegetable oils, animal fats or greases by a transesterification reaction [1,2]. It has been generally considered an adequate alternative fuel for diesel engines as it offers several benefits capable of overcoming the worrying issues related to the environmental quality, energy security, economy growth and social services linked to the use of petroleum fuels, especially in oil-importing countries. Beyond being renewable and biodegradable, biodiesel can be blended in any proportion with petrodiesel to be used in diesel engines with no modification and its combustion emits less greenhouse gases [3–9]. The advantages of biodiesel have incentivized the conception of novel approaches for its production and processing to obtain a fuel with high quality. In this perspective, the study of the thermodynamic properties of biodiesels becomes crucial as they provide strategic information about the procedures one must modify or reformulate to improve the quality of the biodiesel, such that its properties conform with the regulatory standards of the Norm CEN EN 14214 [10] in Europe and the Norm ASTM D6751 in United States of America [11].

Among the most important properties of a fuel, viscosity connotes the fluidity and also affects the quality of the fuel atomization in diesel engines. When using the old mechanical fuel injection systems, higher viscous fuels will certainly block the pump elements, and tend to form large droplets leading to poor fuel atomization and consequent poor engine performance and exhaust emission. Lower viscous fuels, on the opposite, will provoke fuel leakage and cause the fuel pressure to rise more slowly inside the pump [12]. These problems are minimized in the modern "common rail injection systems" that basically use high pressures (up to 200 MPa) to pump the fuel and avoid leakages [12,13]. At this point, the prior knowledge of high-pressure viscosities of

* Corresponding author. Tel.: +351 234401507; fax: +351 234370084.
E-mail address: jcoutinho@ua.pt (J.A.P. Coutinho).

0016-2361/$ - see front matter © 2014 Elsevier Ltd. All rights reserved.
http://dx.doi.org/10.1016/j.fuel.2014.01.031

Table 1
FAMEs composition of the biodiesels studied, in mass percentage.

Methyl esters	S	R	SR
C10:0		0.01	
C12:0		0.04	0.03
C14:0	0.07	0.07	0.09
C16:0	10.76	5.22	8.90
C16:1	0.07	0.20	0.15
C18:0	3.94	1.62	2.76
C18:1	22.96	62.11	41.82
C18:2	53.53	21.07	37.51
C18:3	7.02	6.95	7.02
C20:0	0.38	0.60	0.46
C20:1	0.23	1.35	0.68
C22:0	0.80	0.35	0.46
C22:1	0.24	0.19	0.12
C24:0		0.22	

biodiesels becomes crucial for previewing the engine performance and the quality of emissions.

Most data available in the literature report the temperature dependency of viscosity for biodiesel fuels at atmospheric pressure. Only a few works have focused on measuring and predicting the high-pressure viscosities of biodiesel fuels and their blends with petrodiesel [12–16]. Therefore, this work aims to report new experimental data of high-pressure viscosity for three methylic biodiesels (soybean, rapeseed and their binary mixture) measured at temperatures from 293.15 to 393.15 K and pressures from atmospheric to 140 MPa, and to propose a correlation capable of predicting them and their mixtures with petrodiesel.

2. Experimental section

2.1. Biodiesel samples: synthesis and analysis

The three biodiesel samples here studied: Soybean (S), Rapeseed (R) and their binary mixture (SR) were synthesized in our laboratory by a transesterification reaction of the respective vegetal oils following the procedure described by Pratas et al. [17]. Shortly, the alkaline-catalyzed transesterification reaction was adopted. The molar ratio of oil/methanol used was 1:5 with 0.5% sodium hydroxide by weight of oil as catalyst. The reaction was performed at 55 °C during 24 h under methanol reflux. The reaction time chosen was adopted for convenience and to guarantee a complete reaction conversion. Raw glycerol was removed in two steps, the first after 3 h reaction and then after 24 h reaction in a separating funnel. Biodiesel was purified by washing with hot distillated water until a neutral pH was achieved. Then biodiesel was dried until the EN ISO 12937 limit for water was reached (less than 500 mg/kg of water).

Capillary gas chromatography was used to determine the composition in methyl esters of the biodiesel samples. A Varian CP-3800 with a flame ionization detector in a split injection system with a Select™ Biodiesel for FAME Column, (30 m × 0.32 mm × 0.25 μm), was used to discriminate between all the methyl esters in analysis inclusively the polyunsaturated ones. The column temperature was set at 120 °C and then programmed to increase up to 250 °C, at 4 °C/min. Detector and injector were set at 250 °C. The carrier gas was helium with a flow rate of 2 mL/min. The FAMEs composition of the biodiesels is presented in Table 1.

2.2. Measurement of high pressure viscosity

Experimental measurements of high-pressure viscosities of biodiesels were made using a vibrating-wire instrument [18,19] developed in the TERMOCAL laboratory. This viscometer is capable

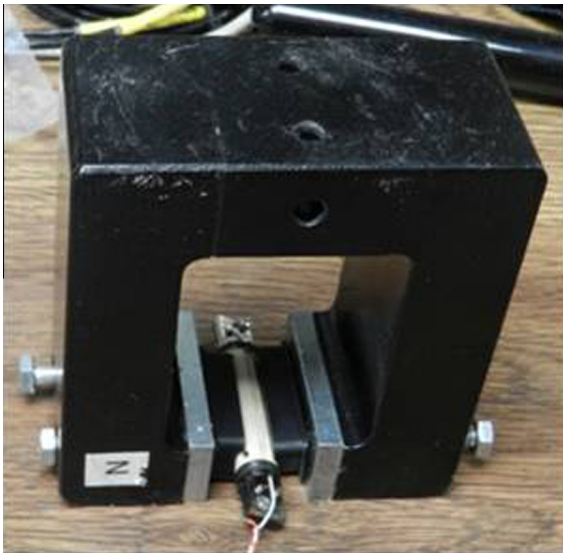

Fig. 1. Picture of the vibrating wire sensor and magnet.

of operating at temperatures between 273.15 K and 423.15 K and at pressures up to 140 MPa. Calibration was performed by means of measurements in vacuum, air, and toluene. The estimated uncertainty of the results is 1% in viscosity. The vibrating wire viscometer has been designed to operate in the viscosity range 0.3–30 mPa s. The main part of the equipment is a sensor with a tungsten wire (length 50 mm and nominal radius 75 μm) anchored at both ends [20], placed inside a pressure vessel, with an external magnetic field orientated in a direction perpendicular to the wire length using magnet placed around the vessel (it can be seen in Fig. 1).

The theory of vibrating-wire viscometer is based on transverse vibration of a stretched wire, which is used to measure the viscosity of the fluid that surrounds the vibrant wire. The oscillations are driven across to induce an alternating current through the wire. The circulation of a constant sinusoidal current through the wire, in combination with the constant magnetic field, generates the vibration of the wire. The electromotive force (EMF) generated through the wire can be measured with a lock-in amplifier (Stanford Research Systems SR830 DSP), which can also provide a constant amplitude sinusoidal drive voltage.

The resonance curve was fitted to the rigorous theoretical model which relates the resonance characteristics of the wire to its physical characteristics as well as the density and viscosity of the surrounding fluid. This experimental resonance curve contains the voltage contribution from the wire motion and the electrical contribution from the effectively stationary wire, and V (the complex voltage sampled by the computer) is expressed as:

$$V = V_1 + V_2 \tag{1}$$

where V_1 is the voltage induced by the wire motion and V_2 is the voltage arising by virtue of passing a current through the impedance of the wire. Both terms are given in Eqs. (2) and (3), respectively.

$$V_1 = \frac{\Lambda f i}{f_0^2 - f^2(1+\beta) + i f^2(\beta' + 2\Delta_0)} \tag{2}$$

$$V_2 = a + bi + cfi. \tag{3}$$

Λ is the amplitude, f is the drive frequency, f_0 and Δ_0 are the resonance frequency and logarithmic decrement in vacuum, β and β' are the additional mass of the fluid and the damping due to the

viscosity of the fluid, the coefficients a, b and c of Eq. (3) account for the electrical impedance of the wire and absorb the offsets set in the lock-in amplifier to ensure that the voltage signal is detected in the most sensitive range.

To fit the experimental and theoretical resonance curves, Eq. (1) in the case of a wire clamped at both ends and immersed in a fluid of known density, six parameters need to be adjusted: the fluid viscosity η, the wire amplitude A, and the background contributions a, b and c. Details of the calculations are given in the literature [19–21].

This instrument is capable of operating at temperatures between 273.15 and 423.15 K and at pressures up to 140 MPa. Calibration was performed by means of measurements in vacuum, air, and toluene. The estimated uncertainty of the results is 1% in viscosity. The vibrating wire viscometer has been designed to operate in the viscosity range 0.3–30 mPa s. The vibrating wire and magnetic assembly were housed in a commercially-available pressure vessel HIP rated for operation at 140 MPa, this vessel was immersed in a bath Hart Scientific 6020. The temperature of the fluid was measured using two platinum resistance thermometers (PRT) and an ASL F100 thermometer. This thermometer was calibrated with an uncertainty of ±0.02 K. The pressure was measured in the external pipework by means of a Druck DPI 104 transducer, with a full scale reading of 140 MPa and an uncertainty of ±0.02% kPa/kPa. The pressure was generated by a HiP pump, model 68–5.75–15.

3. Results and discussion

The experimental viscosities of the three biodiesels here studied are presented in Table 2 where it is seen, as expected, that the magnitude of viscosity is higher for saturated biodiesels at the same temperature and pressure (i.e., biodiesel R is more viscous than biodiesel S) and increases with the pressure due to the increasing molecular interactions as the molecules become more compacted with the pressure rise. Given the similar composition of the fuels here studied, all based on fatty acid methyl esters, is not surprising that all present similar pressure dependencies for the viscosities.

It is also possible to observe that the biodiesel mixture presents higher viscosity values than the separate Soybean and Rapeseed biodiesels. That behavior was already observed in a previously work of ours when measuring viscosities [22], and also in other works addressing the temperature and pressure dependencies of densities [17] and speeds of sound [23] of the Soybean, the Rapeseed and their mixture biodiesels. The biodiesel coming from the combination of the Soybean with the Rapeseed biodiesel presents higher density and speed of sound values than the pure rapeseed or soybean biodiesels.

To model the experimental viscosities presented above we followed an approach similar to that previously proposed by us for the densities and speeds of sound [24]. For that purpose two set of compounds were used to develop a correlation described by Eq. (4)

$$\ln \eta = \ln \eta_0 + a\frac{(P - P_0)}{T^b} \tag{4}$$

with P being the absolute pressure, P_0 the reference pressure in MPa, η the dynamic viscosity at pressure P_0 the viscosity at the reference pressure P_0 in mPa s, T is the absolute temperature in K and a and b the fitting parameters. The experimental data reported by Duncan et al. [13] were used as the training set to adjust the values of the fitting parameters a and b. The validation set was formed by the viscosity data for the three biodiesels here studied (S, R and SR).

Table 2
Experimental high-pressure dynamic viscosity in mPa s for biodiesels S, R and SR.

P (MPa)/T (K)	293.15	313.15	333.15	353.15	373.15	393.15
	Biodiesel S					
0.1	6.33	3.99	2.80	2.13	1.64	1.35
1	6.33	4.01	2.82	2.14	1.65	1.37
5	6.67	4.18	2.94	2.22	1.71	1.45
10	7.11	4.47	3.11	2.32	1.86	1.52
20	8.11	4.94	3.39	2.55	2.03	1.68
30	8.94	5.53	3.81	2.84	2.23	1.83
40	10.0	6.10	4.17	3.12	2.44	1.98
50	11.6	6.70	4.57	3.39	2.67	2.16
60	12.8	7.41	4.98	3.73	2.90	2.32
70	14.6	8.11	5.44	4.05	3.12	2.51
80	16.2	9.00	5.99	4.38	3.31	2.68
100	21.5	10.9	7.02	4.98	3.81	3.03
120	29.9	13.4	8.42	5.68	4.27	3.39
140		16.1	9.95	6.58	4.86	3.76
	Biodiesel R					
0.1	6.93	4.22	2.86	2.11	1.68	1.33
1	6.97	4.27	2.92	2.16	1.68	1.36
5	7.37	4.46	3.02	2.27	1.77	1.41
10	7.75	4.77	3.22	2.37	1.85	1.50
20	9.00	5.32	3.62	2.64	2.07	1.63
30	10.3	5.98	3.93	2.91	2.25	1.80
40	11.6	6.64	4.41	3.21	2.48	1.98
50	12.9	7.33	4.87	3.52	2.73	2.15
60	14.8	8.03	5.33	3.79	2.93	2.34
70	17.3	9.02	5.79	4.19	3.15	2.50
80	19.6	9.99	6.34	4.52	3.37	2.69
100	26.8	11.9	7.53	5.24	3.90	3.07
120		14.8	8.96	5.99	4.49	3.44
140			10.5	6.96	5.06	3.85
	Biodiesel SR					
0.1	6.76	4.20	2.98	2.28	1.78	1.49
1	6.86	4.24	3.03	2.29	1.80	1.51
5	7.24	4.39	3.15	2.40	1.92	1.57
10	7.61	4.65	3.28	2.48	1.99	1.66
20	8.55	5.25	3.65	2.74	2.18	1.83
30	9.88	5.80	4.06	3.01	2.37	1.96
40	10.9	6.45	4.46	3.29	2.60	2.14
50	12.0	7.04	4.82	3.61	2.80	2.32
60	13.4	7.85	5.22	3.87	3.06	2.50
70	15.4	8.75	5.85	4.28	3.28	2.70
80	17.3	9.49	6.32	4.63	3.51	2.85
100		11.3	7.34	5.39	3.96	3.20
120		13.8	8.63	6.10	4.49	3.58
140		17.0	10.2	7.03	5.13	3.93

To assess the predictive ability of the correlation, the relative deviations (RDs) between the predicted and the experimental data of the dynamic viscosity were calculated at different temperatures and pressures according to Eq. (5)

$$RD(\%) = \frac{\eta_{calc_i} - \eta_{\exp_i}}{\eta_{\exp_i}} \times 100 \tag{5}$$

Then the average relative deviation (ARD) was calculated as a summation of the modulus of RD over N_p experimental data points. The overall average relative deviation (OARD) was calculated by Eq. (6), where N_s is the number of systems studied

$$OARD\ (\%) = \frac{\sum_n ARD}{N_s} \tag{6}$$

The values of 1.2 and 0.84 were obtained for parameters a and b, respectively, with which Eq. (4) very well predicts the experimental data, presenting an OARD of only 3.0% for the training set and of 3.9% for the validation set in the temperature range of 293–393 K and pressure range of 0.1–140 MPa, as shown in Table 3. The behavior of the correlation here developed for both sets of compounds can be seen separately in Figs. 2 and 3 for the training and validation sets. The adequacy of this correlation to describe

Table 3
ARDs for the high pressure biodiesels viscosity prediction.

Data reference	Biodiesel	ARD (%)	
		Training set	Validation set
Duncan et al. [12]	Soybean1	3.0	
Duncan et al. [13]	Soybean2	3.6	
	Canola	3.1	
	Canola used	2.9	
	Vistive	2.7	
	Coconut	2.5	
This work	S		3.7
	R		4.7
	SR		3.1
	OARD, %	3.0	3.9

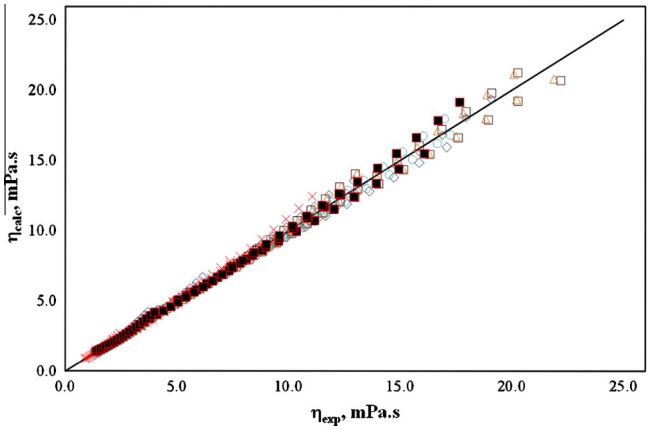

Fig. 2. Experimental and predicted viscosity of the training set for Eq. (1). Soybean1 [12], Canola [13], Canola used [13], Vistive [13], Coconut [13] and Soybean2 [13].

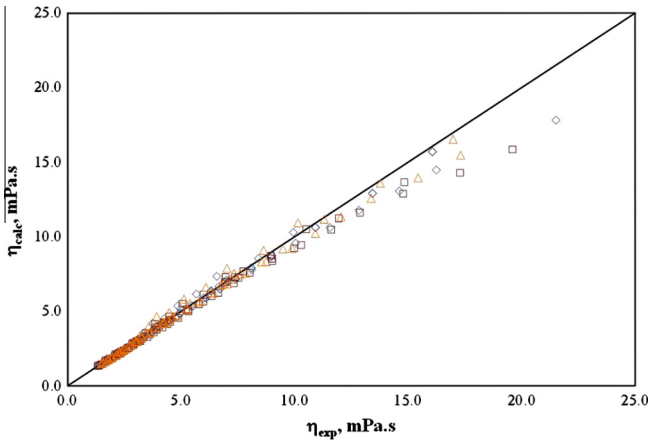

Fig. 3. Experimental and predicted viscosity of the validation set for Eq. (1). S, R and SR.

the pressure dependency of the dynamic viscosity of the biodiesels at different temperatures for the validation set is shown in the Figs. 4–6, where the three biodiesels studied presented high deviations only at the lowest temperature of 293.15 K, while for all the other temperatures the deviations are low. This approach can be easily extended to predict the high pressure viscosities of any biodiesel, provided that the atmospheric pressure values are known either experimentally or can be estimated as we proposed in a previous work [25]. Duncan et al. [13]obtained overall average relative deviations of less than 1% when applying the Tait–Litovitz model to

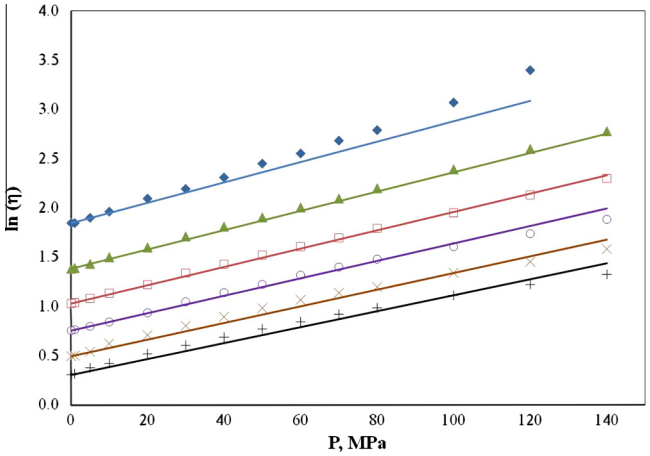

Fig. 4. High-pressure viscosities for biodiesel S at different temperatures. 293.15 K, 313.15 K, 333.15 K, 353.15 K, 373.15 K and + 393.15 K. Lines are the results predicted with the correlation.

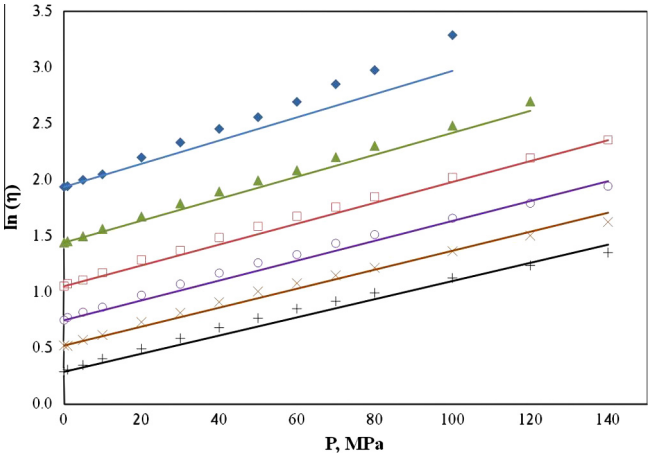

Fig. 5. High-pressure viscosities for biodiesel R at different temperatures. 293.15 K, 313.15 K, 333.15 K, 353.15 K, 373.15 K and + 393.15 K. Lines are the results predicted with the correlation.

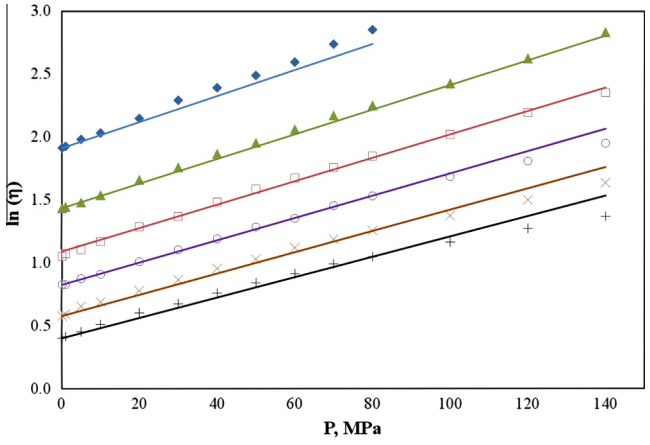

Fig. 6. High-pressure viscosities for biodiesel SR at different temperatures. 293.15 K, 313.15 K, 333.15 K, 353.15 K, 373.15 K and + 393.15 K. Lines are the results predicted with the correlation.

the experimental data reported in their work and here used as training set. The overall deviations obtained for the same data

Table 4
ARDs for the high pressure diesel + biodiesel blends viscosity prediction.

Data reference	Blend	ARD%	
		Volume fraction approach	Molar fraction approach
Duncan et al. [12]	B5	3.2	2.9
	B10	3.6	2.8
	B20	2.6	2.8
	B40	3.0	3.6
	B60	3.6	3.5
	B80	3.5	2.8
	OARD, %	3.3	3.1

set with the correlation proposed in this work are slightly higher (3%) as expected, since the Tait–Litovitz model used by Duncan et al. involves a higher number of parameters correlated from the experimental data than the correlation proposed in this work.

The correlation here developed was also extended to describe mixtures of biodiesels with diesel. To do this, however, a separate parameter fitting of Eq. (4) was done for diesel using the experimental data reported by Duncan et al. [12]. The values of 134.5 and 1.6 were obtained for a and b, respectively. The viscosities of the mixtures were predicted using the Grundberg–Nissan mixing rules expressed by Eq. (7)

$$\ln(\eta_{blend}) = x_{diesel}\ln(\eta_{Diesel}) + x_{biodiesel}\ln(\eta_{biodiesel}) \quad (7)$$

where x_{diesel} and $x_{biodiesel}$ are the mole fractions of diesel and biodiesel in the blended fuel, respectively, and η_{diesel} and $\eta_{biodiesel}$ are the dynamic viscosities of pure diesel and biodiesel at a particular temperature and pressure, respectively. Using Eqs. (4) and (7) together, the prediction of the high-pressure viscosities of the blends was excellent, presenting an OARD of only 3.3% as shown in Table 4. The adequacy of this model can also be seen in Figs. 7–9 for three representative blends (B5, B40 and B80).

In practice, however, the information about the blends of biodiesels with diesel fuel is normally given in volume fractions and sometimes there are no data on the molecular weight and also on the density of the diesel fuel (at different temperatures) to convert the volume fraction into the molar fraction to be used in Eq. (4). An attempt to directly use the volume fraction in the Grundberg–Nissan equation, instead of molar fraction, according to the Eq. (8) to predict the experimental high-pressure viscosities of the blends, where ϕ_{diesel} and $\phi_{biodiesel}$ are the volume fractions of diesel and biodiesel in the blended fuel, respectively, is:

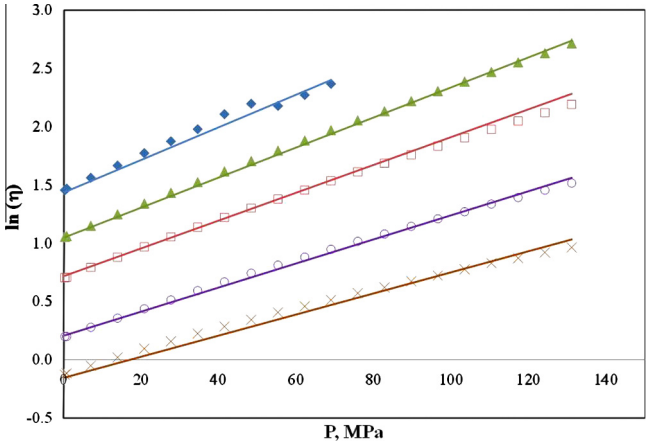

Fig. 7. High-pressure viscosities for B5 at different temperatures. ◆ 283.15 K, ▲ 298.15 K, □ 313.15 K, ○ 343.15 K and × 373.15 K. Lines are the results predicted with the Grundberg–Nissan mixing rules using the molar fraction approach.

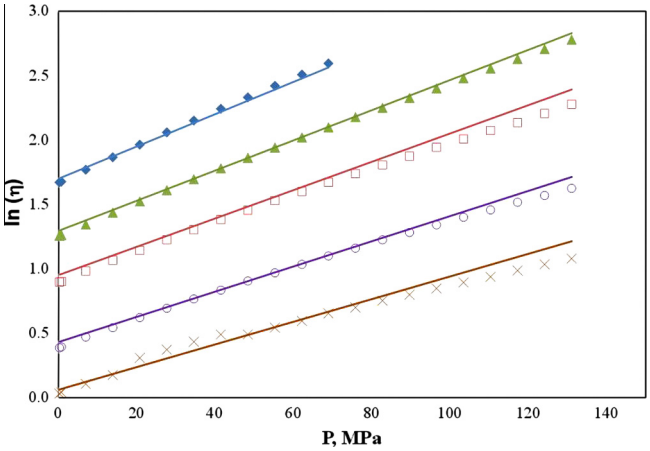

Fig. 8. High-pressure viscosities for B40 at different temperatures. ◆ 283.15 K, ▲ 298.15 K, □ 313.15 K, ○ 343.15 K and × 373.15 K. Lines are the results predicted with the Grundberg–Nissan mixing rules using the molar fraction approach.

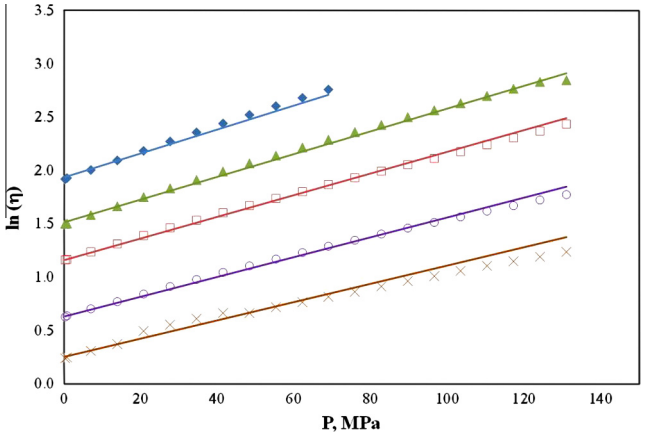

Fig. 9. High-pressure viscosities for B80 at different temperatures. ◆ 283.15 K, ▲ 298.15 K, □ 313.15 K, ○ 343.15 K and × 373.15 K. Lines are the results predicted with the the Grundberg–Nissan mixing rules using the molar fraction approach.

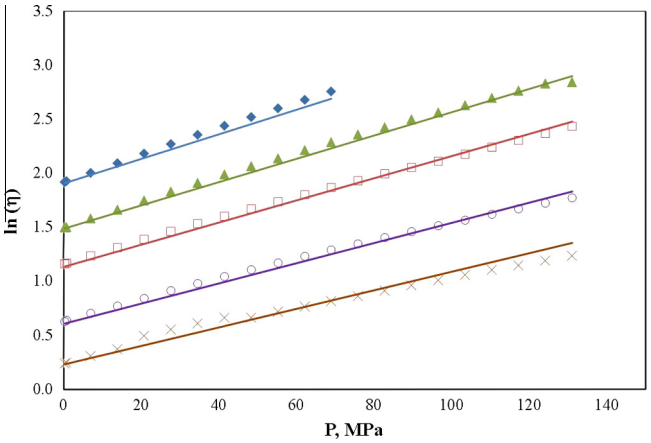

Fig. 10. High-pressure viscosities for B80 at different temperatures. ◆ 283.15 K, ▲ 298.15 K, □ 313.15 K, ○ 343.15 K and × 373.15 K. Lines are the results predicted with the the Grundberg–Nissan mixing rules using the volume fraction approach.

$$\ln(\eta_{blend}) = \phi_{diesel}\ln(\eta_{Diesel}) + \phi_{biodiesel}\ln(\eta_{biodiesel}) \quad (8)$$

The results of the predictions using this approach are similar to those using the molar fraction, suggesting that Eq. (8) may be used to calculate the viscosities of the blends. The ARDS of this approach are presented in Table 4 and its adequacy can also be seen in Fig. 10 for B80.

As expected, and in a similar way to what was observed and discussed above for the biodiesels, due to the use of a larger number of parameters, Duncan et al. [12] obtained lower overall deviations when predicting the viscosity data for the biodiesel/diesel mixtures with the Tait–Litovitz model (the Grundberg–Nissan mixing rules expressed as molar fractions were also used). Nevertheless, the differences in the overall deviations are less pronounced, of 3.3% with the correlation proposed in this work (using the molar fraction approach) and of 2.8% using the Tait–Litovitz model.

4. Conclusions

New experimental data of high-pressure viscosity for three methylic biodiesels, measured at temperatures from 293.15 to 393.15 K and pressures from atmospheric to 140 MPa were here reported and a correlation to predict biodiesels viscosities at high pressures is proposed based on literature data. It is shown that this correlation provides good predictions for the viscosities of the studied biodiesels and, coupled with the Grundberg–Nissan mixing rules, describes very well the experimental data of viscosities for biodiesel fuels blends with diesel, presenting OARDs of 3.9% and 3.3%, respectively. This good description of the data suggests that this correlation can be extended to the prediction of the viscosities of other biodiesel fuels provided that experimental viscosity data at atmospheric pressure is known.

Acknowledgments

Samuel Freitas acknowledges a Ph.D Grant from Fundação para a Ciência e a Tecnologia through his Ph.D. Grant (SFRH/ BD/ 51476/ 2011), Fundação Oriente and also financial support from the University of Aveiro. Mariana B. Oliveira acknowledges Fundação para a Ciência e a Tecnologia for her Post-doctoral Grant (SFRH/BPD/ 71200/2010). CICECO is being funded by Fundação para a Ciência e a Tecnologia through Pest-C/CTM/LA0011/2013.

References

[1] Knothe G, Steidley KR. Kinematic viscosity of biodiesel components (fatty acid alkyl esters) and related compounds at low temperatures. Fuel 2007;86:2560–7.
[2] Dunn RO. Antioxidants for improving storage stability of biodiesel. Biofuels Bioprod Biorefin 2008;2:304–18.
[3] Bozbas K. Biodiesel as an alternative motor fuel: production and policies in the European Union. Renew Sustain Energy Rev 2008;12:542–52.
[4] Van Gerpen J. Biodiesel processing and production. Fuel Process Technol 2005;86:1097–107.
[5] Caresana F. Impact of biodiesel bulk modulus on injection pressure and injection timing. The effect of residual pressure.. Fuel 2011;90:477–85.
[6] Knothe G. Biodiesel derived from a model oil enriched in palmitoleic acid. Macadamia Nut Oil Energy Fuels 2010;24:2098–103.
[7] Anand K, Ranjan A, Mehta PS. Estimating the viscosity of vegetable oil and biodiesel fuels. Energy Fuels 2009;24:664–72.
[8] Demirbas A. New biorenewable fuels from vegetable oils. Energy Sources, Part A Recover Util Environ Eff 2010;32:628–36.
[9] Kerschbaum S, Rinke G. Measurement of the temperature dependent viscosity of biodiesel fuels. Fuel 2004;83:287–91.
[10] CEN; European Committee for Standardization. Automotive fuels – Fatty acid methyl esters (FAME) for diesel engines-Requirements and test methods. E.S.E. EN 14214. Belgium: Brussels; 2003 [n.d].
[11] ASTM: American Society for Testing and Materials Standard D6751. Standard Specification for Biodiesel Fuel Blend Stock (B100) for Middle Distillate Fuels. ASTM: West Conshohocken: PA; 200 [n.d].
[12] Duncan AM, Pavlicek N, Depcik CD, Scurto AM, Stagg-Williams SM. High-pressure viscosity of soybean-oil-based biodiesel blends with ultra-low-sulfur diesel fuel. Energy Fuels 2012;26:7023–36.
[13] Duncan AM, Ahosseini A, McHenry R, Depcik CD, Stagg-Williams SM, Scurto AM. High-pressure viscosity of biodiesel from soybean, canola, and coconut oils. Energy Fuels 2010;24:5708–16.
[14] Robertson LX, Schaschke CJ. Combined high pressure and low temperature viscosity measurement of biodiesel. Energy Fuels 2009;24:1293–7.
[15] Paton JM, Schaschke CJ. Viscosity measurement of biodiesel at high pressure with a falling sinker viscometer. Chem Eng Res Des 2009;87:1520–6.
[16] Chhetri AB, Watts KC. Viscosities of canola, jatropha and soapnut biodiesel at elevated temperatures and pressures. Fuel 2012;102:789–94.
[17] Pratas MJ, Freitas SVD, Oliveira MB, Monteiro SC, Lima AS, Coutinho JAP. Biodiesel density: experimental measurements and prediction models. Energy Fuels 2011;25:2333–40.
[18] Assael MJ, Oliveira CP, Papadaki M, Wakeham WA. Vibrating-wire viscometers for liquids at high pressures. Int J Thermophys 1992;13:593–615.
[19] Peleties F, Trusler JPM. Viscosity of liquid Di-isodecyl Phthalate at temperatures between (274 and 373) K and at pressures up to 140 MPa. J Chem Eng Data 2011;56:2236–41.
[20] Faheem I. PhD thesis. Measurement and prediction of the viscosity of hydrocarbon mixtures and crude oils. London:Imperial College; 2011. p. 85–3 [n.d].
[21] Retsina T, Richardson SM, Wakeham WA. The theory of a vibrating-rod viscometer. Appl Sci Res 1987;43:325–46.
[22] Oliveira MB, Llovell F, Vega LF, Coutinho JAP. Development of simple and transferable molecular models for biodiesel production with the soft- SAFT equation of state. submitted to Chem Eng Res Des. 2013.
[23] Freitas SVD, Paredes MLL, Daridon J-L, Lima ÁS, Coutinho JAP. Measurement and prediction of the speed of sound of biodiesel fuels. Fuel 2013;103:1018–22.
[24] Habrioux M, Freitas SVD, Coutinho JAP, Daridon JL. High pressure density and speed of sound in two biodiesel fuels. J Chem Eng Data 2013;58:3392–8.
[25] Freitas SVD, Pratas MJ, Ceriani R, Lima AS, Coutinho JAP. Evaluation of predictive models for the viscosity of biodiesel. Energy Fuels 2011;25:352–8.